ISSN 1560-0904, Polymer Science, Series B, 2018, Vol. 60, No. 3, pp. 395–404. © Pleiades Publishing, Ltd., 2018.

COMPOSITES

Lab Scale Study on Humidity Sensing and D.C. Conductivity of Polypyrrole/Strontium Arsenate ($Sr_3(AsO_4)_2$) Ceramic Composites[1]

Sangappa K. Ganiger[a],* and M. V. Murugendrappa[b],**

[a] *Department of Physics, Government Engineering College, Raichur-584134, Karnataka, India*

[b] *Department of Physics, Centre of Excellence in Advanced Materials Research, BMS College of Engineering, Bangalore-560019, Karnataka, India*

**e-mail: sangappaganiger1973@gmail.com*

***e-mail: murugendrappamv.phy@bmsce.ac.in*

Received June 23, 2017;
Revised Manuscript Received October 31, 2017

Abstract—In-situ polymerization of pyrrole was carried out with strontium arsenate (ceramics) in the existence of oxidizing agent ammonium persulphate to synthesize polypyrrole/strontium arsenate composites by chemical oxidation method. The polypyrrole/strontium arsenate composites were synthesized with various compositions viz., 10 to 50 wt % of strontium arsenate was placed in polypyrrole. The surface morphologies of these composites were analyzed using Scanning Electron Microscopy (SEM) which confirmed the embedment of strontium arsenate particles in PPy chain. The Fourier Transform Infra-Red spectra (FTIR) revealed the shift of lengthens frequencies towards elevated frequency area. The powder X-ray diffraction patterns (XRD) disclosed the crystalline behavior exhibition of the composites. Thermographs of thermal analysis (TG/DTA) exposed the stronger stability of polypyrrole/strontium arsenate composites than PPy. D.C. conductivity reveals that, the strontium arsenate concentration in polypyrrole is accountable for the variant of conductivity of the composites. The results of the study signify the increment of D.C. conductivity for 40 wt % of strontium arsenate in polypyrrole. The temperature reliant conductivity dimension shows the thermally activated exponential behavior of PPy/$Sr_3(AsO_4)_2$ composites. The reduction in electrical resistance was experienced, when the polymer composites were bare to the wide range of relative humidity (Rh) (from 30 to 95%). This reduce is due to enhance in surface electrical conductivity ensuing from humidity fascination and also due to capillary abridgment of water causing change in conductivity within the sensing materials. The composite shows sensitivity in the range 30 to 95% Rh, we also studied response and recovery time.

DOI: 10.1134/S1560090418030119

INTRODUCTION

This study is conducted with the aim of preparing a PPy/$Sr_3(AsO_4)_2$ composite by chemical oxidation method. Its characteristics, enhanced conductivity and humidity sensitivity are examined. Now a day's humidity management and monitoring is of huge attention in various areas like, fresh and wrap up foodstuff, drug cargo space and ecological control for precious antiques [1, 2]. Commercial humidity sensors consist of dew point, infrared, catalytic and tin oxide sensors, which may be luxurious, or have to soaring temperature process and devour significant quantity of power and towering cost of preservation [3]. Currently the investigation is alert on the expansion of the D.C. conductivity material which is also humidity sensor [4–6]. Various types of conducting polymers, such as polypyrrole, polythiophene and polyaniline, which are used for humidity and gas sensing purposes, are studied and now for the sake of better performance of these sensors, the advanced research is under progress [7–9]. Recompense with polymers as sensing materials are their light weight, flexibility, stumpy cost and easy process of manufacture [10]. Pure polymer, polymer blends and polymer–inorganic composites have also been deliberate for the same purposes, have also been deliberated for the same purposes, having been ensued in dissimilar degree of advancements in this area [11–19]. In general, conducting polymers perform fairly equally on revelation to humidity. A resistance reduce is observed owing to the configuration of H-bonding among water molecules and the nitrogen centre of the polymer backbone, make easy the proton exchange to enlarge the doping level of the conducting polymer thus increasing the amount of charge carri-

[1] The article is published in the original.

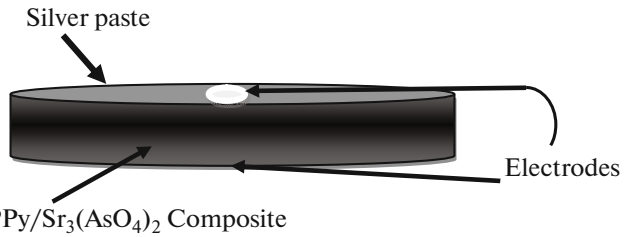

Scheme 1.

ers, consequentially increasing the conductivity [20]. In the present paper we report the detailed investigation of D.C conductivity and humidity sensing response of $PPy/Sr_3(AsO_4)_2$ composites.

EXPERIMENTAL

Synthesis of $PPy/Sr_3(AsO_4)_2$ Composite

The pyrrole was sterilized by distillation under abridged pressure. Pyrrole solution 0.3 M is placed in a beaker which was positioned in an ice tray mounted on a magnetic stirrer. The oxidizing agent of ammonium persulphate solution of 0.6 M was constantly added drop-wise with the assist of a burette to the over stated pyrrole solution. The reaction was permitted for 5 hours under constant stirring by maintaining a temperature in the range of 0 to 5°C. The precipitated polypyrrole was filtered and dried in hot air oven at 100°C, yielding the polypyrrole of 3.6 g. For such 0.3 M pyrrole solution, 0.36 g (resulted from 10% weight of PPy) of sodium metavanadate ($Sr_3(AsO_4)_2$) was added and assorted meticulously maintaining the same physical conditions as mentioned above. To this solution 0.6 M ammonium persulphate was constantly added drop wise with the assist of a burette, from which $PPy/(Sr_3(AsO_4)_2)$ (10%) composite was obtained.

The same procedure was adopted and 20% (by weight of PPy) mounted 0.72 gram, 30% (by weight of PPy) mounted 1.08 g 40% (by weight of PPy) mounted 1.44 gram and 50% (by weight of PPy) mounted 1.8 g of $Sr_3(AsO_4)_2$ (Sisco Research Lab Ltd.) was added for 0.3 M pyrrole solution which produced the $PPy/Sr_3(AsO_4)_2$ composite powder. Using hydraulic press the pure PPy and $PPy/Sr_3(AsO_4)_2$ composites powder were pressed in the form of pellets of 1 cm diameter as seen in Scheme 1. D.C conductivity of this composite was analyzed by measuring the current values with respect to voltage from room temperature to 200°C.

Characterization

The surface morphology of pure PPy, $PPy/Sr_3(AsO_4)_2$ (40%) composite and $Sr_3(AsO_4)_2$ were studied by Scanning electron microscope (SEM) images. The Fourier Transform Infra Red (FTIR) spectra for the pure PPy, $PPy/Sr_3(AsO_4)_2$ (40%) nano composite and strontium arsenate were recorded through the spectrometer in KBr medium at room temperature to study the characteristic stretching frequencies. The X-ray Diffractometer (XRD) patterns for the pure PPy, $PPy/Sr_3(AsO_4)_2$ (weight 40%) composite and $Sr_3(AsO_4)_2$ were studied on using CuK_α radiation (λ = 1.5418 Å) in the 2θ range 20°–80° to understand the characteristic peak of amorphous PPy. Thermal gravimetric (TG)/Differential Thermal Analysis (DTA) studies were made in the assorted temperature from 40 to 740°C at 10 deg/min for the pure PPy, $PPy/Sr_3(AsO_4)_2$ (40%) composite and strontium arsenate ($Sr_3(AsO_4)_2$).

Measurements

The temperature dependent conductivity was recorded using two-probe method on a Keithley–2000 multimeter, USA. The sample in the pellet form was used for humidity sensing. The planar resistance of the sensor was recorded at the room temperature by controlling the humidity in a glass compartment as shown in Scheme 2. The humidity in the chamber was first lowered by using mechanical drier, later on proscribed water vapors at room temperature were then commenced gradually for increasing the humidity within the compartment from 30 to 95% Rh. Relative humidity within the compartment was observed and measured by a usual pre-calibrated humidity meter (Mextech-DT-615).

RESULTS AND DISCUSSION

SEM Analysis

The individual granules observed had a close packing nearly spherical shape. Such spherulites grow one above the other and thus form an unbroken structure; the dimensions of these spherulites vary. However the spongy morphological feature made it considerably difficult in distinguishing the granules from one another, forming a much closed packed structure. Such morphological textures are believed to be fine for the applications of sensing. The SEM image of prepared polypyrrole is shown in Fig. 1a, most of the particles are spherical in nature which appears as globule structures or "cauliflower" structures, this is a well-documented morphology [21] typical of the bulk polypyrrole. The globules are made up of micro-spherical grains has been observed.

The particle size of strontium arsenate ($Sr_3(AsO_4)_2$), has the immense size of the particles in comparison with pure PPy. The SEM images of $Sr_3(AsO_4)_2$ is seen in Fig. 1b.

The micrograph of the polypyrrole/strontium arsenate composite ($PPy/Sr_3(AsO_4)_2$) is represented in Fig. 1c. The size of the particle is depicted in the vari-

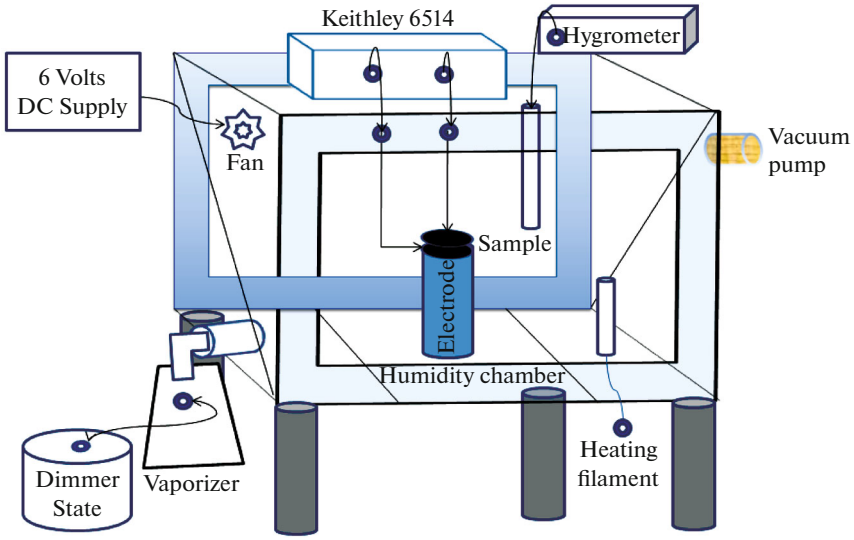

Scheme 2 (Color online).

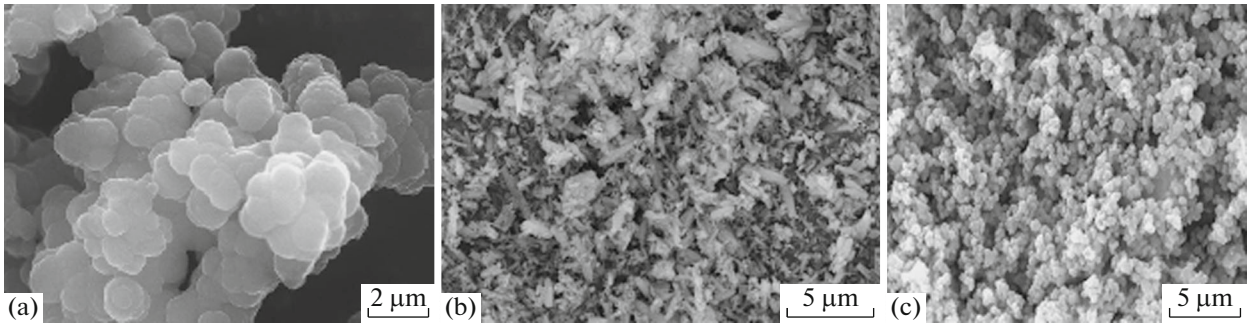

Fig. 1. SEM micrograph of (a) the pure PPy, (b) $Sr_3(AsO_4)_2$, (c) PPy/$Sr_3(AsO_4)_2$ (40 wt %) composite.

ous wt % combinations which show the decrease in the particle size. This enhancement in the particle size can be compared with the particle size of pure PPy which is due to uniform blending of strontium arsenate particles in polypyrrole chain because of fragile inter-particle contact. Figure 1c shows SEM image of prepared $Sr_3(AsO_4)_2$ dispersed polypyrrole composite. The particles are spherical in shape in the nano range. Most of the particles highlighted the weak interaction between dispersed oxide materials in polypyrrole which is believed to enhance the crystallinity. This confirms the formation of the polymer composite. The SEM representation also reveals the presence of $Sr_3(AsO_4)_2$ in polypyrrole which is homogeneously distributed throughout the polymer sample. The particles of size ranging from 210 to 300 nm are observed in the composite. The SEM representation also reveals the presence of $Sr_3(AsO_4)_2$ in polypyrrole, which is homogeneously distributed throughout the polymer samples. The particle size of $Sr_3(AsO_4)_2$ has immense in size comparison with pure PPy [22]. The needle shaped particles of varying size are observed, which shows the netted compact structure. Usually such particles lead to the betterment of the properties especially in storage system applications. The particles of size ranging from 180 to 250 nm are observed in the figure.

FTIR Analysis

The Fourier Transfer Infra Red (FTIR) spectra for pure PPy studied. The characteristic frequencies were empirical at 1710, 1560, 1480, 1330, 1210, 1130, 1050, 910, 627, and 619 cm^{-1}, for pure PPy as seen in Fig. 2a. The intense peaks at 1710, 1210, and 910 cm^{-1} may be accredited due to the occurrence of C=N stretching, N–H bending deformation and C–N stretching frequencies respectively. Figure 2b shows FTIR spectrum of $Sr_3(AsO_4)_2$ sample. The observation of spectrum shows peaks at 856, 702, and 613 cm^{-1} this is due to metal–oxygen (M–O) bending nature. The peaks at 1770 and 1200 cm^{-1} may attribute the overtones. Peaks around 3450 may be due to water and hydrogen.

Figure 2c shows FTIR spectrum of $Sr_3(AsO_4)_2$ dispersed polypyrrole composite. This spectrum shows the peaks of metal oxides below 1000 cm^{-1}. Some additional peaks around 1000 to 2000 cm^{-1} may be due to polypyrrole, this is comparable with FTIR of pure polypyrrole. Thus the spectrum shows the peaks of $Sr_3(AsO_4)_2$ and polypyrrole, confirming the formation of polymer composite. A paradigm of 40 wt% had its characteristic frequencies for polypyrrole/strontium arsenate composite (PPy/$Sr_3(AsO_4)_2$) (40 wt %) composite were observed at 1707, 1563, 1476, 1393, 1201, 1113,1051, 930, 793, 685, and 619 cm^{-1} as seen. From this outcome it can be attributed that, the occurrence of C=N stretching, N–H bending distort, C–N stretching and C–H bending distort frequencies were reallocated towards superior frequency side for the PPy/$Sr_3(AsO_4)_2$ (40 wt %) composite. This shows, the uniform allotment of $Sr_3(AsO_4)_2$ particles in the polymeric chain due to the Vander Waal interface between the PPy chain and $Sr_3(AsO_4)_2$. Other composites of PPy with 10, 20, 30, and 40 wt % of $Sr_3(AsO_4)_2$ had the nearly same IR spectra of absorption peaks with hardly any variation in their stretching frequency [23–25].

XRD Analysis

Figure 3a shows X-ray diffraction outline of polypyrrole. cautiously analysis of X-ray diffraction of polypyrrole imply that it has amorphous nature with a wide peak centered approximately 2θ ~25°. Figure 3b shows XRD pattern of pure $Sr_3(AsO_4)_2$. The peaks corresponding to 2θ = 25.40°, 31.30°, 36.62°, 44.72°, and 47.80° are due to (006), (110), (202), (205) and (1 0 10) planes of $Sr_3(AsO_4)_2$ (JCPDS 13–0261) with the inter-planar spacing d = 3.50, 2.85, 2.45, 2.04, and 1.90 Å respectively. These peaks correspond to rhombohedral crystalline nature of strontium arsenate. Figure 3c shows XRD pattern of polypyrrole/strontium arsenate composite (PPy/$Sr_3(AsO_4)_2$) composites. On comparison of XRD pattern of $Sr_3(AsO_4)_2$, pure polypyrrole and polypyrrole/$Sr_3(AsO_4)_2$ composites, the composite pattern shows peaks of the both $Sr_3(AsO_4)_2$ and polypyrrole. In addition to this, the shift of some peaks of both samples confirms formation of polymer composite. Some $Sr_3(AsO_4)_2$ peaks have not appeared in the composite because of some of the particles are masked in the polymer matrix. The scattering from PPy chains at the inter-planar spacing results in the development of broad peaks [26]. It is seen from XRD outline of polypyrrole/strontium arsenate 40 wt % composite, the rhombohedral peak of $Sr_3(AsO_4)_2$ indicates the crystalline nature of the composite. By contrasting the XRD pattern of these composite with that of $Sr_3(AsO_4)_2$, the major peaks corresponding to 2θ = 26.73°, 29.71°, 32.45°, 36.10°, and 44.96° are due to (006), (015), (110), (202), and (205) planes (JCPDS 13–0261) of $Sr_3(AsO_4)_2$ with interplanar distance d = 3.32, 3.00, 2.75, 2.48, and 2.01 Å respectively. By contrasting the XRD patterns of these composite and $Sr_3(AsO_4)_2$, it is inveterate that strontium arsenate has keep its structure even though it is dispersed in polypyrrole during polymerization reaction [26].

TG/DTA Analysis

Figure 4a shows TG/DTA graph for the pure PPy from the TG/DTA curve, loss of weight at 0.052 mg/min is observed at 64.9°C is due to the vaporization of water in the polypyrrole and loss of weight is 0.064 mg/min is observed at 240.5°C which is ascribed to the degradation of the polymer chain with respect to total weight of the sample 4.057 mg Fig. 4b shows TG/DTA graph for strontium arsenate. For strontium arsenate, a peak observed at weight loss of 0.049 mg/min at 204°C is due to the volatilization of tiny molecules present. The thermal study shows the compound is stable up to 204°C. Figures 4c shows TG/DTA graph for polypyrrole/strontium arsenate composites. As a paradigm polypyrrole/strontium arsenate (40 wt %) composite had its main peaks observed at around 78.5°C is due to the vaporization of water in the composite and weight loss of 0.216 mg/min at 268.4°C is due to the degradation of the polymer composite with esteem to whole weight of the taster 6.508 mg. The decomposition temperature of the PPy/$Sr_3(AsO_4)_2$ composites was found to depend on the amount of $Sr_3(AsO_4)_2$ particles present in the composite. The trend of degradation for the PPy/$Sr_3(AsO_4)_2$ composites is similar to that of PPy, and also presents two-steps weight loss process. The decomposition temperature is changes as the amount of $Sr_3(AsO_4)_2$ particle changes in the composites, which shows the higher stability of the PPy/$Sr_3(AsO_4)_2$ composites [27, 28].

D.C. Conductivity Study

The behavior of D.C. conductivity as a function of temperature is studied for polypyrrole/strontium arsenate composites. The D.C. conductivity of polypyrrole/strontium arsenate composites were studied for the influence of temperature. Conductivity is dependent on temperature, because as temperature increases the charges will thermal gain energy and moves to conduction band since these composites behaves like a semiconductors. The increase in conductivity is due to the increase of efficiency of charge transfer between $Sr_3(AsO_4)_2$ and polymer chains with increase in temperature. It is also suggested that the thermal curling affects the chain alignment of the polymer, which leads to the increase of conjugation length and which in turn brings about the increase of conductivity. Also, there will be molecular rearrangement on heating, which make the molecules favorable for electron delocalization. The temperature dependence of the con-

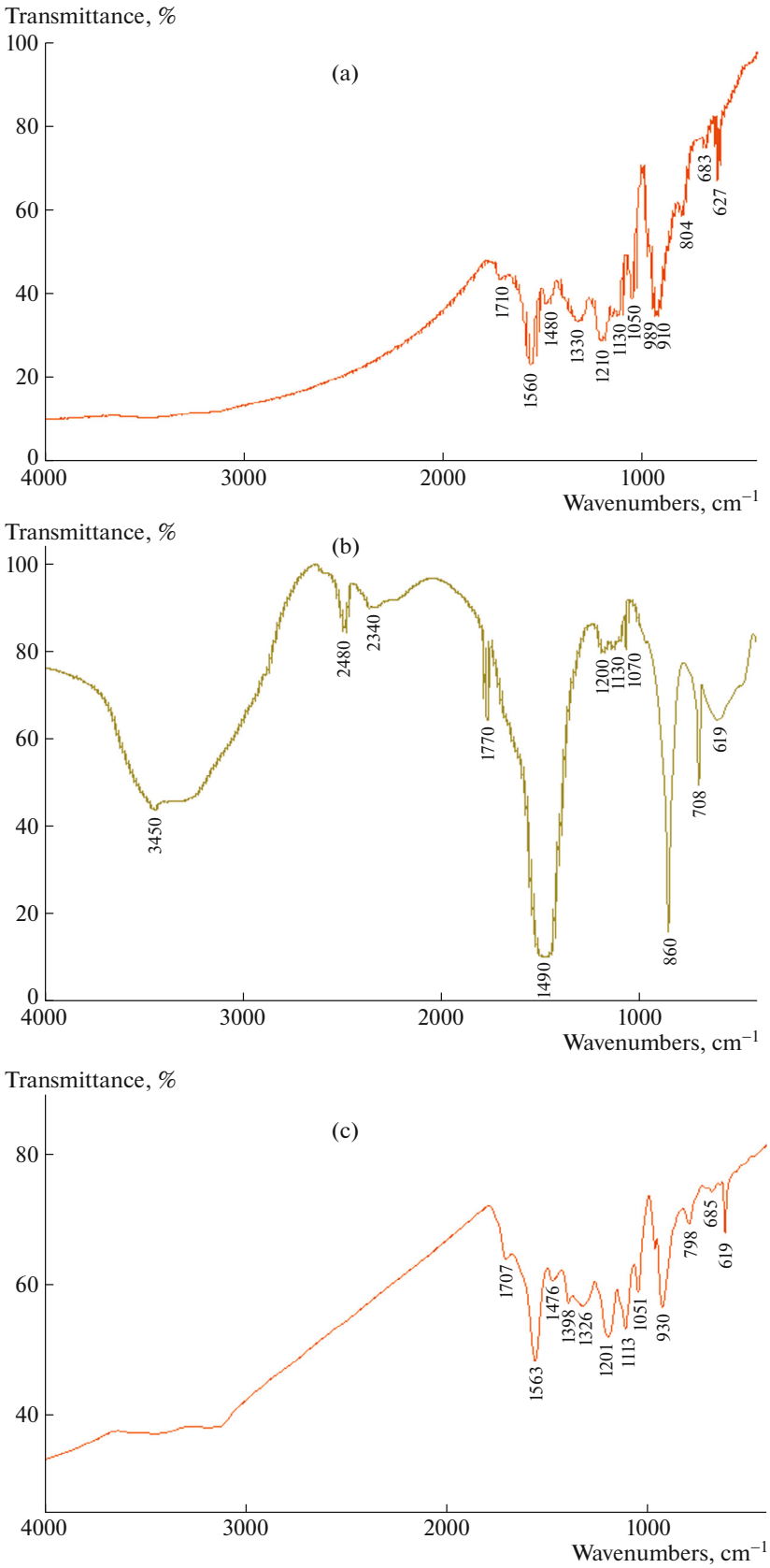

Fig. 2. (Color online) FTIR spectrum of (a) pure PPy, (b) $Sr_3(AsO_4)_2$, (c) PPy/$Sr_3(AsO_4)_2$ (40 wt %) composite.

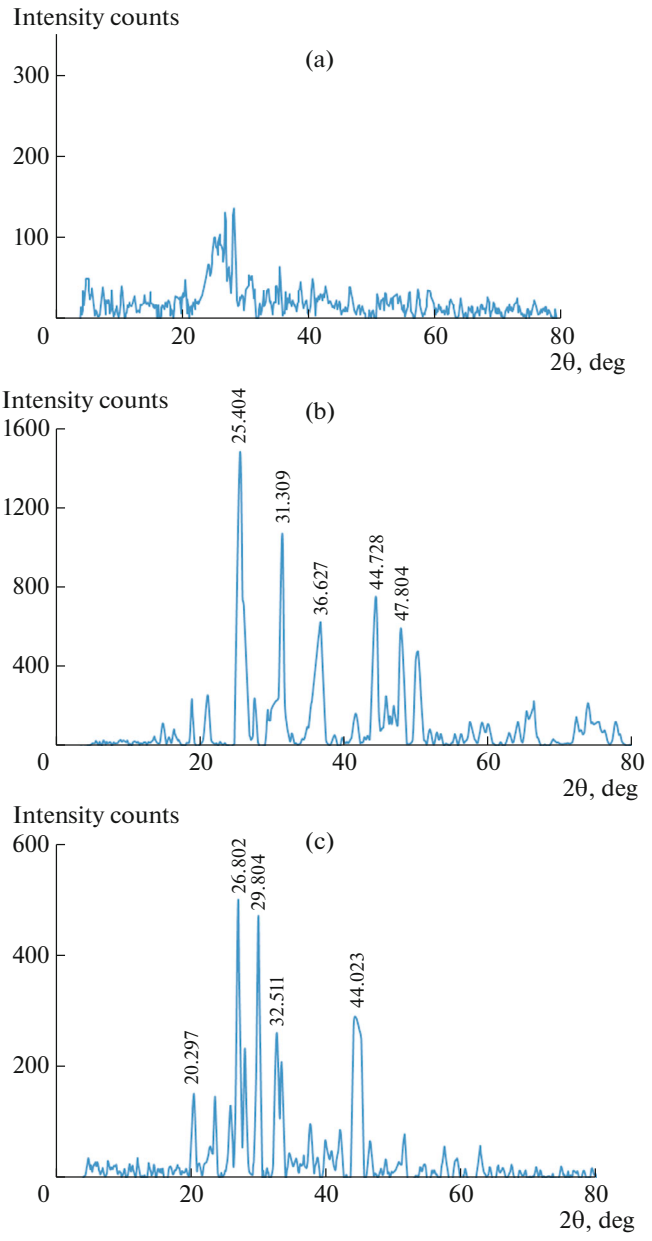

Fig. 3. (Color online) XRD pattern of (a) pure PPy, (b) $Sr_3(AsO_4)_2$, (c) PPy/$Sr_3(AsO_4)_2$ (40 wt %) composite.

ductivity for conducting polymers is expressed by a variable range hopping (VRH) model proposed by Mott. According to this model, the behavior of electronic conduction in disordered and non-metallic materials is controlled by the thermally assisted hopping of electrons between localized states and is given by,

$$\sigma(T)\alpha \exp[-T_0/T^{1/(n-1)}], \quad (1)$$

$$kT_0 = \lambda\alpha^3/\rho_0, \quad (2)$$

where α is the coefficient of exponential decay of the localized states, ρ_0 is the density of states at the Fermi level and λ is a dimensional constant. However, many models have predicted as $\sigma\alpha T^{-1/2}$.

Figure 5a represent the study outcomes of the composite. All the weight percentages from 10 to 50 remained mostly horizontal, hardly there was any conduction observed for the temperatures between 30 to 110°C. For the weight percentage of 20, 30, and 40 conductivity increased exponentially from 110 to 200°C. The exponential relational was observed right at 110°C for weight percentage of 40, while for the weight percentages 20 and 30 it was observed from 140°C. For the weight percentage of 10 hardly any conductivity was observed until 160°C, later on exponential relation between conductivity and weight percentage was observed.

The response of weight percentage was studied for the D.C. conductivity with respect to temperature. Figure 5b show the variant of D.C. conductivity as a function of weight percent of strontium arsenate in pure polypyrrole.

At 50 and 100°C, all the weight percentages from 10 to 50 remained neutral without responding for the conductivity. For 150°C, the conductivity was inversely proportional for the weight percentages between 10 to 20. The scarce conductivity was noticed between weight percentages 20 to 30. Conductivity linearly increased between the weights percentages 30 to 40. In contrast to this the trend inversed between the weight percentages 40 to 50. For 200°C inverse trend of conductivity was noticed between the weight percentages 10 to 30, while the conductivity is being linearly shoot up between the weight percentages of 30 to 40. Once again the trend inversed between the weight percentages 40 to 50. 40 wt % of $Sr_3(AsO_4)_2$ in polypyrrole showed a percolation threshold. It can be seen that the values of conductivities remains constant for all the composites except 40 wt % of $Sr_3(AsO_4)_2$ in polypyrrole. This may be owing to the widespread chain length of polypyrrole which aid the hopping of charge carriers while the content of strontium arsenate is 40 wt %. Further the reduce in conductivity is observed after 40 wt % which might be ascribed owing to the allocation of $Sr_3(AsO_4)_2$ particles of bigger grain size which are partly blocking the hopping of charge carriers between the favorable localized sites.

Humidity Sensing Properties

Figure 6a shows the change in resistance versus percentage relative humidity of PPy/$Sr_3(AsO_4)_2$ composites. The relative humidity is approximately linear in between 30 and 95%.

The reduce in the resistance or enhance in the conductivity with rising humidity can be ascribed to the trapping of water molecule in the annulled formed in between polymer and $Sr_3(AsO_4)_2$ particles. At stumpy humidity, the trapping of the water molecules is fewer therefore; the polymer chains would be liable to curl

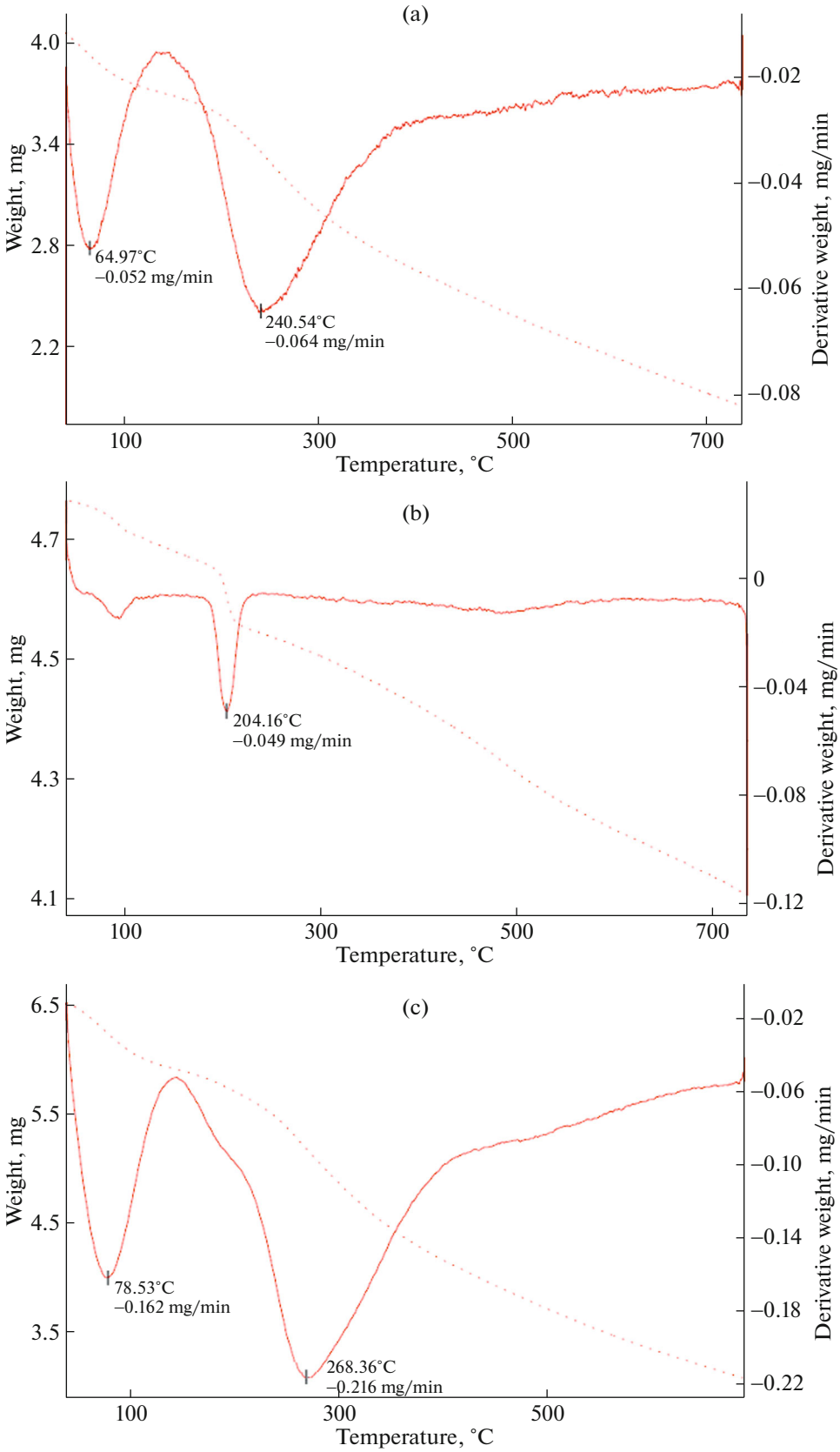

Fig. 4. (Color online) TG/DTA micrograph of (a) pure PPy, (b) $Sr_3(AsO_4)_2$, (c) PPy/$Sr_3(AsO_4)_2$ (40 wt %) composite (dotted lines—weight, solid lines—derivative weight).

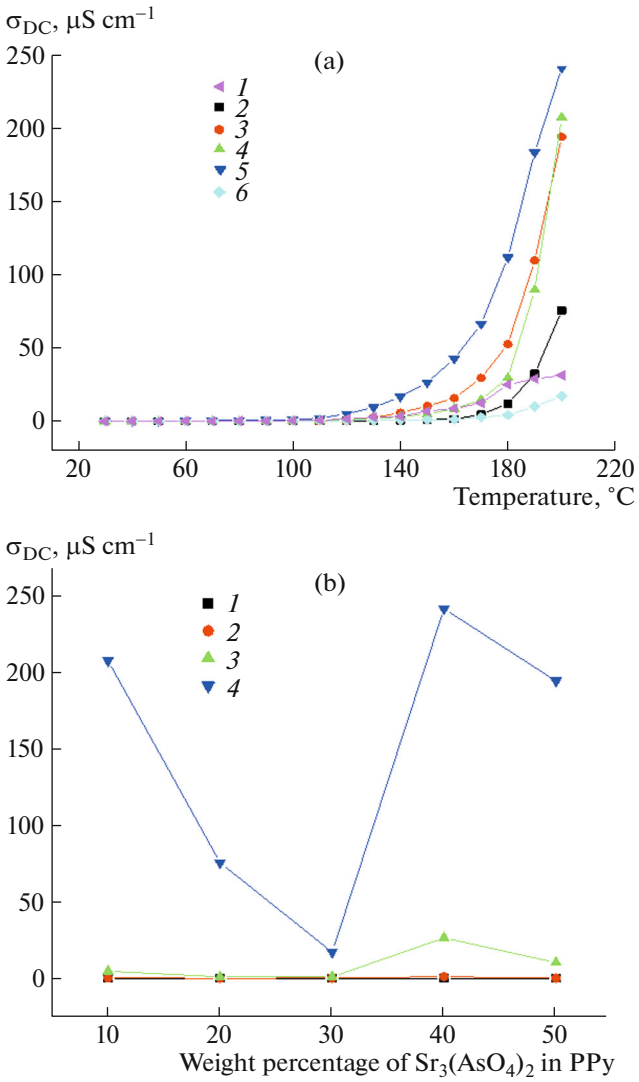

Fig. 5. (Color online) Variation of D.C conductivity (a) as a function of temperature for the PPy/$Sr_3(AsO_4)_2$ composite with (*1*) 0, (*2*) 10, (*3*) 20, (*4*) 30, (*5*) 40, (*6*) 50 wt % of $Sr_3(AsO_4)_2$; (b) as a function of wt % of $Sr_3(AsO_4)_2$ in PPy at (*1*) 50, (*2*) 100, (*3*) 150, (*4*) 200°C.

up into compact coil form. On the contrary, at elevated humidity, the polymer absorbs water molecules, and the polymer chains swells, followed by the uncurling of the compact coil for into straight chains that are aligned with respect to each other. This geometry of the polymer is favorable for elevated sensitivity. Among all PPy/$Sr_3(AsO_4)_2$composites, 40 wt % shows huge change in resistance followed by 20, 50, 30, and 10 wt %. This nature of the polymer is favorable for improved mobility of the $Sr_3(AsO_4)_2$ ion or the charge transfer across the polymer chains thus increasing the conductivity [29]. All the composites have shown the considerable diminution in resistance with increase in relative humidity, indicating it's potentiality as a polymer based humidity sensor.

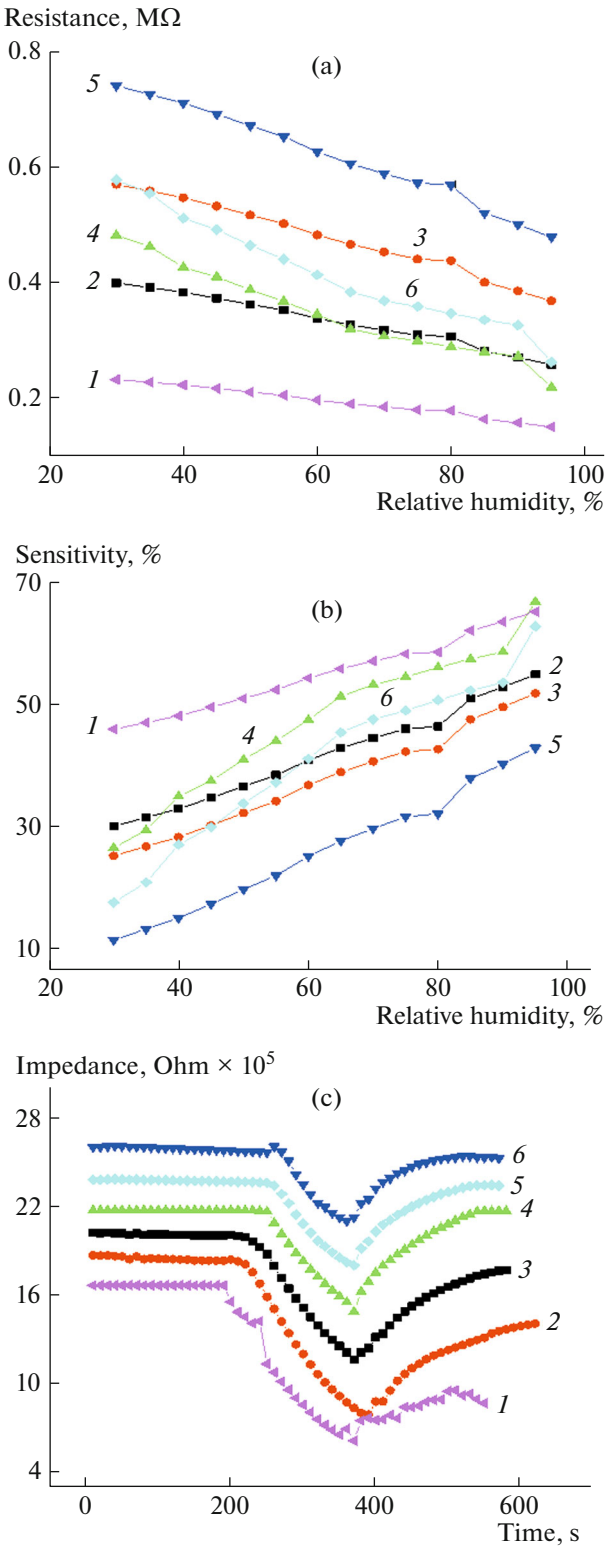

Fig. 6. (Color online) (a) Resistance as a function of (a) percentage relative humidity, (b) variation of percentage sensitivity as a function of percentage relative humidity, (c) response and recover curves as a function of time at various percentages relative humidity of PPy/$Sr_3(AsO_4)_2$ composites at different weight percentages: (*1*) 0, (*2*) 10, (*3*) 20, (*4*) 30, (*5*) 40, and (*6*) 50 wt %.

The variation of sensitivity plotted against % RH for PPy/$Sr_3(AsO_4)_2$ composites are shown in Fig. 6b. Maximum sensitivity is obtained for PPy/$Sr_3(AsO_4)_2$ composites of 30 wt %. The relative humidity is almost linear in between 30 and 95%. The decrease in the resistance or increase in the conductivity with increasing humidity can be attributed to the trapping of water molecule in the voids formed in between polymer and $Sr_3(AsO_4)_2$ particles. It is clearly seen that PPy/$Sr_3(AsO_4)_2$ composite shows a linear response from 30 to 95% RH. On the other hand, PPy, 30 wt % composites the sensitivity varies from 25 to 68% where as it is from 10 to 62% for PPy, 10, 20, 40, and 50 wt % composites. Thus, 30 wt % composite shows better sensing properties and exhibits good linearity in sensing response curve. These composites obey percolation theory at different weight percentages; the sensitivity of percentage humidity finding is as equated below

$$S = \frac{RH_2 - RH_1}{RH_1} \times 100,$$

where RH_1 and RH_2 are the sample's resistivity for humidity, at level 1 and 2 respectively.

Figure 6c show the response and recovery curves corresponding to water adsorption and desorption process for 10, 20, 30, 40, and 50 wt % of PPy/$Sr_3(AsO_4)_2$ composites. The average response time of PPy/$Sr_3(AsO_4)_2$ composite is 150 seconds and the recovery time is 200 seconds as the humidity changes from 30 to 95% RH this can be attributed to the lower grain boundary [30]. The response time and recovery time of the above composites prove that the above composite can efficiently function as good humidity sensing material.

CONCLUSIONS

An attempt is made in this study on humidity sensing and electrical properties of PPy/$Sr_3(AsO_4)_2$ composites synthesized by chemical oxidation technique. The characterization results such as SEM shows the formation of vague surface morphology with capillary pores which proves its suitability for its application in humidity sensing. The XRD spectrum of composites shows the presence of prominent peaks, indicating the crystalline nature of composite despite polypyrrole being amorphous. The FTIR spectrum reveals the formation of composites due to the strong interactions between polypyrrole chains and $Sr_3(AsO_4)_2$ particles. The electrical properties in these composites show a strong dependence on content of $Sr_3(AsO_4)_2$ in PPy. The composite with 40 wt % of $Sr_3(AsO_4)_2$ in PPy shows pronounced reduction in resistivity indicating the potential of this material to be used for D.C. conductivity. All the wt % of PPy/$Sr_3(AsO_4)_2$ composites showed the linear inverse relation with Rh when compared with the pure PPy which had no such linear inverse relation. The PPy/$Sr_3(AsO_4)_2$ humidity sensor shows a high sensitivity, fast response (150 s), and rapid recovery (200 s) characteristics in the humidity range of ~33–95% RH, when compared with the pure PPy which had no such linear inverse relation, while the response and recovery time for PPy/$Sr_3(AsO_4)_2$, respectively.

ACKNOWLEDGMENTS

The authors would like to acknowledge The Principal, BMSCE, Bengaluru-560019 and Dr. Guruprasad Hugar, Asst. Prof. of GEC Raichur for their cooperation and help. Author would express his gratitude towards Sophisticated Analytical Instruments Facility (SAIF) of Cochin University of Science and Technology, Cochin, India, for facilitating the analysis through FTIR, TGA, SEM and XRD. The Authors also thank World Bank funded project Centre of Excellence on Advanced Materials Research under TEQIP 1.2.1.

REFERENCES

1. *Handbook of Conducting Polymers,* 3rd ed., Ed. by T. A. Skotheim and J. R. Reynolds (CRC Press, Boca Raton, 2006).
2. J. L. Bredas and G. B. Street, Acc. Chem. Res. **18**, 309 (1985).
3. G. Inzelt, J. Solid State Electrochem. **15**, 1711 (2011).
4. R. Strümpler and J. Glatz-Reichenbach, J. Electroceram. **3**, 329 (1999).
5. A. K. Bakhshi, Bull. Mater. Sci. **18**, 469 (1995).
6. R. Ansari, E.-J. Chem. **3**, 186 (2006).
7. B. V. Chaluvaraju, S. K. Ganiger, and M. V. Murugendrappa, Int. J. Latest Technol. Eng. Manage. Appl. Sci. **3** (5), 33 (2014).
8. M. V. Murugendrappa and M. V. N. Ambika Prasad, J. Appl. Polym. Sci. **103**, 2797 (2007).
9. Zh. A. Boeva, O. A. Pyshkina, and V. G. Sergeev, Polym. Sci., Ser. A **54**, 614 (2012).
10. M. V. Murugendrappa, S. Khasim, and M. V. N. Ambika Prasad, Bull. Mater. Sci. **28**, 565 (2005).
11. B. V. Chaluvaraju, S. K. Ganiger, and M. V. Murugendrappa, Int. J. Innovative Sci. Eng. Technol. **1** (4), 141 (2014).
12. J. Hou, G. Zhu, and J. Zheng, Polym. Sci., Ser. B **53**, 546 (2011).
13. Q. Luo, X. Li, D. Wang, Y. Wang, and J. An, J. Mater. Sci. **46**, 1646 (2011).
14. L. Ai and J. Jiang, J. Mater. Sci.: Mater. Electron. **21**, 410 (2010).
15. S. Hossein Hosseini and A. Ali Entezami, Iran. Polym. J. **14**, 201 (2005).
16. O. Nakamura, I. Ogino, and T. Kodama, Solid State Ionics **3–4**, 347 (1981).
17. C. D. Doyle, Anal. Chem. **33**, 77 (1961).
18. J. C. Aphesteguy and S. E. Jacobo, J. Mater. Sci. **42**, 7062 (2007).

19. B. V. Chaluvaraju, S. K. Ganiger, and M. V. Murugendrappa, Int. J. Eng. Sci. Res. Technol. **3** (10), 314 (2014).
20. S. A. Kumar, A. Pratap Singh, P. Saini, F. Khatoon, and S. Dhawan, J. Mater. Sci. **47**, 2461 (2012).
21. A. Ben Slimane, M. M. Chehimi, and M.-J. Vaulay, Colloid Polym. Sci. **282**, 314 (2004).
22. N. Parvatikar, S. Jain, S. Khasim, M. Revansiddappa, S. V. Bhoraskar, and M. V. N. Ambika Prasad, Sens. Actuators, B **114**, 599 (2006).
23. N. Perinka, M. Držková, M. Hajná, B. Jašúrek, P. Šulcová, T. Syrový, M. Kaplanová, and J. Stejskal, J. Therm. Anal. Calorim. **116**, 589 (2014).
24. B. V. Chaluvaraju, S. K. Ganiger, and M. V. Murugendrappa, Polym. Sci., Ser. B **56**, 935 (2014).
25. Z. Chen and C. Lu, Sens. Lett., **3**, 274 (2005).
26. S. K. Ganiger, B. V. Chaluvaraju, and M. V. Murugendrappa, Int. J. Innovative Res. Sci. Eng. Technol. **4** (7), 5819 (2015).
27. M. L. Singla, S. Awasthi, and A. Srivastava, Sens. Actuators, B **127**, 580 (2007).
28. M. Wan, Z. Wei, Z. Zhang, L. Zhang, K. Huang, and Y. Yang, Synth. Met. **135–136**, 175 (2003).
29. B. V. Chaluvaraju, S. K. Ganiger, and M. V. Murugendrappa, Int. J. Macromol. Sci. **5**, 1 (2015).
30. A. A. A. De Queiroz, D. A. W. Soarez, P. Trzesniak, and G. A. Abraham, J. Polym. Sci., Part B: Polym Phys. **39**, 459 (2001).